Dexmedetomidine alleviates LPS-induced acute lung injury via regulation of the p38/HO-1 pathway

YINGYING SUN, YIN XIA, XINGHUI LIU, JUNXIA LIU, WEITIAN HE, HONGWU YE and XIANREN YUAN

Department of Anesthesiology, Anhui Provincial Children's Hospital of Anhui Medical University, Hefei, Anhui 230051, P.R. China

Received November 22, 2019; Accepted May 27, 2020

DOI: 10.3892/mmr.2020.11330

Abstract. Acute lung injury (ALI) is a common critical illness in clinical anesthesia and the intensive care unit that can cause acute hypoxic respiratory insufficiency. Despite various therapeutic regimes having been investigated, there is currently no effective pharmacotherapy available to treat ALI. Previous studies have reported that the NOD-like receptor protein 3 (NLRP3) signaling pathway plays an important role in the inflammatory response and is involved in the pathogenesis of ALI. Moreover, dexmedetomidine (Dex), an α2-adrenergic receptor activating agent, has been routinely used as an adjuvant therapy in treating inflammatory diseases, including ALI. However, the precise pathological mechanisms of Dex in ALI remain to be elucidated. Thus, the present study aimed to investigate the effects of the p38/heme oxygenase 1 (HO-1) signaling pathways in the pathological mechanisms of Dex in ALI. Newborn male Sprague-Dawley rats (n=48) were randomly divided into four groups (n=12 each), and an intravenous injection of lipopolysaccharide (LPS) was used to successfully induce the ALI model, with increased pulmonary damage, cell apoptosis, interleukin-1β (IL-1β) secretion and edema fluid in lungs. Moreover, the mRNA and protein expression levels of NLRP3 were significantly upregulated, while that of HO-1 were downregulated by LPS treatment. Furthermore, the levels of phosphorylated p38 were also upregulated in ALI rats. It was demonstrated that Dex administration significantly alleviated LPS-induced ALI, downregulated the secretion of IL-1β, decreased the expression of NLRP3, inhibited the phospho-activation of p38 and increased HO-1 expression. In addition, pharmacological inhibition of p38 using the inhibitor SB20380 further enhanced the effect of Dex. Collectively, these preliminarily results identified the effects of Dex intervention on the pathogenesis of ALI via the regulation of p38/HO-1 signaling pathways, which impacted the inflammatory effects, thus providing a theoretical basis and novel evidence for the development of new targets for clinical treatment of ALI.

Correspondence to: Dr Yingying Sun, Department of Anesthesiology, Anhui Provincial Children's Hospital of Anhui Medical University, 39 Wangjiang East Road, Hefei, Anhui 230051, P.R. China
E-mail: liyh1081@163.com

Key words: acute lung injury, dexmedetomidine, NOD-like receptor protein 3, interleukin-1β, p38, heme oxygenase 1

Introduction

Acute lung injury (ALI) is a common critical illness in clinical anesthesia and the intensive care unit (ICU) (1-3). ALI refers to the injury of pulmonary capillary endothelial cells and alveolar epithelial cells during non-cardiac diseases, such as severe infection, shock, trauma and burns, and can cause diffuse pulmonary interstitial and alveolar edema, which can lead to acute hypoxic respiratory insufficiency or failure (4). Moreover, the development of ALI to the severe stages can result in acute respiratory distress syndrome (ARDS) (5,6); ALI/ARDS seriously threaten the lives of patients, affecting quality of life and increasing the economic burden. Compared with older children and adults, infants have smaller airways, increased incomplete alveolar vascular bed development, improved chest wall elasticity and lower functional residual capacity, and thus are a high-risk group of ALI/ARDS (7). Children have high chest wall compliance, low rib support to the lungs, and difficulty in maintaining negative intrathoracic pressure. As a result, the residual volume of lung function is reduced, which is a disadvantageous factor in acute lung injury. Furthermore, the overall mortality rate of ALI in pediatrics is 18-27%, and the mortality rate of ARDS is 29-50% (8,9). Any response of the lung to the injurious stimulus may be mediated by several pathways, depending on the cause of injury. For instance, bacterial antigens trigger the inflammatory response by activating Toll-like receptors (TLR) (10), and chemical injury may induce damage to cell membrane and oxidative stress, leading to the activation of intracellular kinases (11,12). Although the development of intensive care medicine has made progress worldwide, the understanding and treatment status of ALI/ARDS remains unsatisfactory. Therefore, it is of great clinical significance to elucidate the pathogenesis of ALI/ARDS and develop targeted drugs to effectively prevent or treat the disease. As an α2-adrenergic receptor agonist, dexmedetomidine (Dex) has an analgesic effect and is widely used for sedation and anesthesia in patients with ICU

ventilator support; however, there are few studies related to the progression of Dex and ALI. Our previous clinical study reported that Dex can reduce the occurrence of delirium during postoperative recovery by reducing the level of inflammatory response (13); however, the detailed underlying signaling mechanisms remain to be elucidated.

The NOD-like receptor protein 3 (NLRP3) signaling pathway plays an important role in the inflammatory response and is involved in the pathogenesis of ALI/ARDS (14-17). Moreover, NLRP3 is composed of NLRs and caspase-1 and is widely present in T cells, B cells, monocytes, macrophages, dendritic cells and granulocytes (18,19). In the absence of an activating substance, the leucine-rich repeat domain of NLRP3 binds to the NACHT domain, inhibiting self-oligomerization and destabilizing the inactive state (20,21). There are numerous substances that activate NLRP3, including lipopolysaccharide (LPS) bacterial toxin, extracellular ATP or necrotic cellular components (22). Furthermore, the activated NLRP3 inflammasome provides a platform for cytokines, including interleukin (IL)-1, IL-6, IL-18 and IL-33, which are subsequently converted into activated IL-1β, IL-6, IL-18 and IL-33 states (23,24).

Heme oxygenase 1 (HO-1) plays a key role in regulating organ protection from ischemia-reperfusion injury (25). In addition, the nuclear factor erythroid 2-related factor 2 (Nrf2)/HO-1 signaling pathway plays an important role in preventing the occurrence of ALI/ARDS, and activation of Nrf2 reduces the severity of ALI/ARDS (26). The activation of the Nrf2/HO-1 signaling pathway also inhibits the activation of NLRP3 inflammasome, thus reducing IL-1β expression and exerting anti-inflammatory and cytoprotective effects (27,28). p38 kinase, which is a member of the mitogen-activated protein kinase (MAPK) family, plays a central role in inflammatory responses in a variety of disease models, such as Parkinson's disease, cancer and inflammatory disease (29-31), and has been the subject of basic research and drug discovery (32). Furthermore, inhibition of p38 activation has been revealed to suppress LPS-induced inflammation in different situations, such as in LPS-induced inflammation in IPEC-J2 cells, bronchial epithelial cells, macrophages and rats (29,33-35).

In the present study, it was hypothesized that Dex may activate the HO-1 signaling pathway by suppressing p38 to mediate the anti-inflammatory effect in LPS induced ALI. Therefore, the activity of NLRP3 may be inhibited by Dex, which could reduce IL-1β secretion and the level of inflammatory response in Sprague-Dawley rats with ALI. Therefore, the present study may provide a theoretical basis and novel evidence for the discovery of new targets for clinical treatment of ALI.

Materials and methods

Animal model of ALI and experimental groups. Newborn male specific pathogen-free Sprague-Dawley rats (age, 7 days; weight, 250-300 g) were provided by Experimental Animal Center of Anhui Medical University (no. SCXK-2017-023). Rats were housed in standard laboratory cages under standard housing conditions of 12 h light/12 h dark cycles at a temperature of 22±2˚C, along with free access to food and water, and all animal experiments were performed in accordance with the international standards on animal welfare, as well as being compliant with the committee of Anhui Medical University.

The rats (n=48) were randomly divided into four groups (n=12 rats each) (36,37): i) Saline control group; ii) LPS (cat. no. L2630-100MG; Sigma Aldrich; Merck KGaA) group; iii) LPS and Dex (cat. no. MB1434-S-100MG; Dalian Meilunbio Biology Technology Co., Ltd.) group; and iv) Dex and SB203580 [cat. no. 5633S; Cell Signaling Technology, Inc. (CST)] group. The rats were anesthetized with an intraperitoneal injection of 40 mg/kg pentobarbital sodium (cat. no. 1063180500; Merck KGaA). The rats were tracheal intubated with a micro-atomizer and the control group was given 300 μl physiological saline, the experimental group was administered LPS (5 mg/kg) in 300 μl physiological saline, which was fully administered via a nebulizer at an oxygen flow-rate of 4 L/min for 25 min. The rats were normally fed without intubation for 30 min after each 6 h intubation. Then, 12 h later, rats were sacrificed by decapitation, bronchoalveolar lavage and lung tissue were assessed, after which they underwent thoracotomy. The right bronchus was ligated, and the right lung tissue specimen was isolated for preparation for subsequent experiments.

Morphological analysis of the lungs. The fresh lung samples were weighed for wet mass after harvesting or dried overnight at 75˚C for dry mass measurement (38). Haematoxylin and eosin (H&E) staining was used to observe histological pulmonary structures and the condition of inflammation following exposure to LPS. After harvesting at the assigned time points, the lungs were imaged and fixed in 4% paraformaldehyde at room temperature for 12 h, dehydrated, embedded in paraffin wax and serially sectioned at 5-μm. The sections were stained with haematoxylin for 20 min and eosin for 15 min at room temperature. The sections were imaged using a fluorescence microscope (Olympus IX50; Olympus Corporation) linked to the NIS-Elements F3.2 software (Nikon Corporation). The airspace volume density was measured by dividing the sum of the airspace area by the total area (39). In total, ≥3 randomly selected images from five samples were assessed per group at the assigned time point.

Immunohistochemistry. Immunostaining was performed on paraffin transverse sections against IL-1β and NLRP3 (40). Transverse sections of rat lungs were fixed by carnoy solution (1:500) at room temperature for 3 h, de-waxed in xylene, rehydrated (100, 90 and 70% ethanol), heated in a microwave at 92-98˚C for 15 min for antigen retrieval before exposure to the primary antibody with citrate buffer (pH=6.0) and serially sectioned at 5 μm. Next, the sections were immersed in 3% hydrogen peroxide for 10 min to block endogenous peroxidase. Non-specific immunoreactions were blocked using 5% inactivated goat serum (Gibco) in PBS for 30 min at room temperature. The sections were washed in PBS and incubated with NLRP3 (1:250; cat. no. ab263899; Abcam) and IL-1β (1:200; cat. no. ab9722; Abcam) antibodies overnight with shaking at 4˚C. For immunohistochemistry, following extensive washing, the sections were incubated in horseradish peroxidase (HRP)-conjugated goat anti-rabbit IgG secondary antibody (1:400; cat. no. E030120; EarthOx Life Sciences) for 2 h at room temperature in a dark box, and were then

subsequently stained with 3'3-diaminobenzidine at room temperature for 5 min (Fuzhou Maixin Biotech Co., Ltd.). After immunostaining, the sections were counterstained with haematoxylin at room temperature for 10 min and observed using an IX50 confocal microscope (Olympus Corporation; magnification, x200).

TUNEL analysis. TUNEL staining was performed using an *In Situ* Cell Death Detection kit (Roche Diagnostics) according to the manufacturer's instructions. Sections were fixed with 4% paraformaldehyde for 20 min at 20˚C. Sections (thickness, 4 μm) were deparaffinized in xylene by heating at 60˚C, rehydrated in decreasing concentrations of ethanol (100, 95, 90, 80 and 70%) and heated for antigen retrieval at 37˚C. Endogenous peroxidase was blocked in 3% hydrogen peroxide. Then, three different dilutions (1:7, 1:11 and 1:16) of terminal deoxynucleotidyl transferase in reaction buffer (containing a fixed concentration of digoxigenin-labelled nucleotides) were applied to serial sections at 37˚C for 1 h before the slides were placed in stop/wash buffer for 10 min. Following intensive washing, a pre-diluted anti-digoxigenin peroxidase-conjugated antibody (1:2; cat. no. 11207733910; Roche Diagnostics) was applied for 30 min at room temperature. For immunofluorescent staining, the sections were incubated with the corresponding Alexa Fluor 488 secondary antibody (1:1,000; cat. no. A-11029; Invitrogen; Thermo Fisher Scientific, Inc.) at room temperature for 2 h in a dark box. All sections were then counterstained with DAPI (1:1,000; Invitrogen; Thermo Fisher Scientific, Inc.) at room temperature for 30 min. Sections were mounted with Prolong Gold Antifade mounting media containing DAPI (Invitrogen; Thermo Fisher Scientific, Inc.). Stained cells were observed in five randomly selected fields of view. The presence of TUNEL$^+$ cells was determined using Image Analysis Software V.2.4.2 (Olympus Corporation). The percentage of TUNEL$^+$ cells relative to the total cells in the same area between the control and experimental groups was evaluated (n=8 lungs for each group).

Western blotting. Western blotting was performed in accordance with a standard procedure using polyclonal antibodies that specifically recognized phosphorylated (p)-p38, p38, HO-1 and NLRP3. The methods for protein extraction and immunoblotting used in this study have been described previously (40). Protein samples were extracted from lung tissue homogenate using a RIPA buffer (Sigma-Aldrich; Merck KGaA) supplemented with protease and phosphatase inhibitors, and the protein concentrations were quantified using the bicinchoninic acid assay. The extracted protein samples were separated by SDS-PAGE on a 10% gel, and subsequently transferred onto a PVDF membrane (EMD Millipore). The membrane was blocked with 5% non-fat milk at room temperature for 1 h and incubated with antibodies against p38 (1:500; cat. no. 8690; CST), p-p38 (1:500; cat. no. ab4822; Abcam), HO-1 (1:500; cat. no. 82206; CST) and NLRP3 (1:500; cat. no. ab214185; Abcam) in TBS buffer at 4˚C overnight. GAPDH was used as a loading control (1:1,000; cat. no. 5174; CST). After incubation with the secondary antibodies at room temperature for 1 h, which were either HRP-conjugated goat anti-rabbit IgG (1:3,000; cat. no. E030120; EarthOx Life Sciences) or HRP-conjugated goat anti-mouse IgG (1:3,000; cat. no. E030110; EarthOx Life Sciences), the blots were developed with the SuperSignal™ West Femto Chemiluminescent Substrate (Thermo Fisher Scientific, Inc.) and Gel Doc™ XR+ System (Bio-Rad Laboratories, Inc.). The intensity of the bands was analyzed using the Quantity One software V.4.6.7 (Bio-Rad Laboratories, Inc.), according to the manufacturer's instructions. The western blotting results are representative of three independent experiments.

ELISA. Briefly, the left lung was lavaged three times with 500 μl saline via tracheal catheter to obtain bronchoalveolar lavage (BAL) fluid. BAL fluid was centrifuged at 4˚C at 600 x g for 10 min. The supernatant was stored at -20˚C until further examination. The level of secreted IL-1β in BAL fluid was detected using a Rat IL-1β ELISA kit (cat. no. ab100704; Abcam), according to the manufacturer's instructions.

RNA isolation and reverse transcription-quantitative PCR (RT-qPCR). Total RNA was isolated from fresh rat lung tissue or MLE-12 cells (American Type Culture Collection) stored on ice using the E.Z.N.A® Total RNA kit (Omega Bio-Tek, Inc.), according to the manufacturer's instructions. Total RNA was reverse transcribed into cDNA at 42˚C for 15 min and 85˚C for 5 sec using the PrimeScript™ RT Reagent kit (Takara Bio, Inc.). Subsequently, qPCR was performed using SYBR® Green qPCR assay (Thermo Fisher Scientific, Inc.). All the specific primers used are described in Table I (41-43). qPCR was performed in the Bio-Rad S1000TM thermocycler (Bio-Rad Laboratories, Inc.), with the following qPCR thermocycling conditions: Initial denaturation at 95˚C for a 3 min, followed by 40 PCR cycles (95˚C for 5 sec, 60˚C for 20 sec and 72˚C for 20 sec), using ABI 7000 RT PCR machines. Corresponding relative mRNA expression was calculated by the $2^{-\Delta\Delta Cq}$ method (44) and normalized to β-actin. The qPCR results are representative of three independent experiments.

Data analysis. Data analysis and the construction of statistical graphs were performed using GraphPad Prism 5 software package (GraphPad Software, Inc.). Data are presented as the mean ± SEM from ≥3 independent experiments. ANOVA (followed by Tukey's post hoc test) or an unpaired Student's t-test were used to analyze whether there were any significant differences between the control and treatment groups. $P<0.05$ was considered to indicate a statistically significant difference.

Results

LPS exposure induces ALI. The histological characteristics of the H&E stained transverse sections of the lungs were compared between the control and LPS groups (Fig. 1A). The integrity of the structure of alveoli before LPS exposure was identified by examination of pathological tissue sections. After LPS exposure, diffuse damage was observed in the alveoli, alveolar sacs, alveolar tubes, alveolar septa and bronchi. Moreover, there were numerous inflammatory cells in the alveolar septa of the LPS group (Fig. 1A). Furthermore, LPS treatment significantly increased the number of TUNEL$^+$ pulmonary cells in lungs of the LPS group compared with the control (Fig. 1B and C), indicating that LPS promoted apoptosis in the pulmonary cells. IL-1β plays an important

Table I. Primers used for reverse transcription-quantitative PCR.

Gene	Primer sequence (5'-3')
HO-1	F: CGTGCAGAGAATTCTGAGTTC
	R: AGACGCTTTACGTAGTGCTG
p38	F: AGGGCGATGTGACGTTT
	R: CTGGCAGGGTGAAGTTGG
NLRP3	F: GGGACTCAAGCTCCTCTGTG
	R: GAGGCTCTGGTTATGGGTCA
GAPDH	F: AGCCACATCGCTCAGACA
	R: TGGACTCCACGACGTACT

F, forward; R, reverse; HO-1, heme oxygenase 1; NLRP3, NOD-like receptor protein 3.

role in the body's inflammatory response and is involved in the pathogenesis of ALI. With collected rat bronchoalveolar lavage, using ELISA kits, it was demonstrated that the secretion levels of IL-1β in the bronchoalveolar lavage fluid were significantly upregulated upon LPS exposure (Fig. 1D).

In addition, the quantity of the wet lung and dry lung in the control group and LPS group was weighed. It was indicated that the wet-to-dry weight ratio of the LPS group was significantly higher compared with the control group, which suggested that a large amount of edema fluid was accumulated in the alveolar and interstitial lungs in the LPS group (Fig. 1E). Collectively, the results demonstrated the successful establishment of the ALI model in rats and that LPS induced severe injury in the lungs.

p38/HO-1 signaling pathway is involved in the regulation of NLRP3. p38 plays a central role in the inflammatory response, and to further assess the possible underlying mechanisms of the LPS-induced ALI in rat lungs, the expression levels of inflammatory factors were measured by immunohistochemistry, RT-qPCR and western blotting. NLRP3 inflammasome is a critical component of the innate immune system, and is upregulated when the lungs are injured. The immunohistochemistry (Fig. 2A and B), western blotting (Fig. 2C and D) and RT-qPCR (Fig. 2E) results suggested that the mRNA and protein expression levels of NLRP3 were significantly upregulated upon LPS exposure in lungs. Moreover, western blotting results demonstrated that LPS induced the upregulation of p-p38 expression (Fig. 2C and D). However, there were no significant differences ($P>0.05$) in the expression of p38 between the two groups (Fig. 2C and D).

HO-1 is reported to be a downstream effector of p38, and activation of p38 suppresses the anti-inflammatory effect of HO-1 (45). Thus, the present study determined the expression of HO-1 in ALI, and it was found that both the mRNA and protein expression levels of HO-1 were significantly downregulated after LPS exposure in lungs (Fig. 2C-E). Thus, LPS exposure induced the activation of p38, the downregulation of HO-1 and the upregulation of NLRP3.

Dex and pharmacological inhibition of p38 co-operate to suppress ALI. Our previous results revealed that Dex can reduce the level of inflammatory response (13); however, the role of Dex in ALI remains to be elucidated. Thus, Dex administration was given to LPS-induced ALI model rats. Moreover, inflammation and morphological changes were examined by H&E staining, and the integrity of alveoli structure before LPS exposure was observed by examination of pathologic tissue sections (Fig. 3A). Furthermore, diffuse damage was observed in the alveoli, alveolar sacs, alveolar tubes, alveolar septa and bronchi after LPS exposure, and there was considerable lymphocyte infiltration in the pulmonary interstitium (Fig. 3A). However, the addition of Dex reversed LPS-induced inflammation and morphological damage in the lungs (Fig. 3A). It was demonstrated that LPS induced p38 activation (Fig. 2), and thus it was further investigated whether inhibition of p38 attenuated ALI, using SB203580 (p38 MAPK inhibitor) in the group exposed to LPS and Dex. Compared with the group exposed to Dex and LPS, the occurrence of inflammation and morphological damage was further inhibited by suppressing p38 signaling pathway with SB203580 (Fig. 3A). Furthermore, Dex administration in the LPS group reversed LPS-induced upregulation of NLRP3 expression in the lungs, and this effect could be further enhanced by SB203580 (Fig. 3B and C). Bronchoalveolar lavage was collected and the concentration of inflammatory factor IL-1β was measured by ELISA, the data showed the secretion of IL-1β demonstrated the same trend as NLRP3 expression (Fig. 3D). Therefore, it was speculated that Dex inhibited ALI, which was further enhanced by p38 suppression.

Dex alleviates ALI via inhibition of the p38 signaling pathway. As pharmacological inhibition of p38 enhanced the effect of Dex in ALI, whether Dex function upstream or parallel to the p38 pathway was assessed by detecting its mRNA and protein expression levels by RT-qPCR and western blotting, respectively. Compared with the control group, the phosphorylation level of p38 was significantly suppressed by Dex, while addition of SB203580 further enhanced this effect. Moreover, the mRNA and protein expression levels of NLRP3 were suppressed by Dex, and further reduced by SB203580 treatment (Fig. 4A and C). The LPS-induced decrease in HO-1 expression was reversed by Dex, and the addition of SB203580 further increased HO-1 expression (Fig. 4A-C). Collectively, the results indicated that Dex alleviated ALI by suppressing p38 activation and inducing HO-1 expression.

Discussion

ALI is a serious complication of critical illness and clinical anesthesia, however, the underlying mechanisms remain to be elucidated. The present results suggested that LPS exposure could lead to ALI. Furthermore, it was speculated that LPS activated p38, which subsequently suppressed HO-1 signaling, promoted the expression of NLRP3 and induction of IL-1β, and finally resulted in lung damage. Moreover, it was demonstrated that Dex could prevent ALI by inhibiting p38 activation, rescuing the expression of HO-1 signaling and decreasing NLRP3; these signal pathway interactions are summarized in a schematic diagram (Fig. 4D).

It has been reported that systemic diseases caused by various pathogenic factors in the lungs and outside the

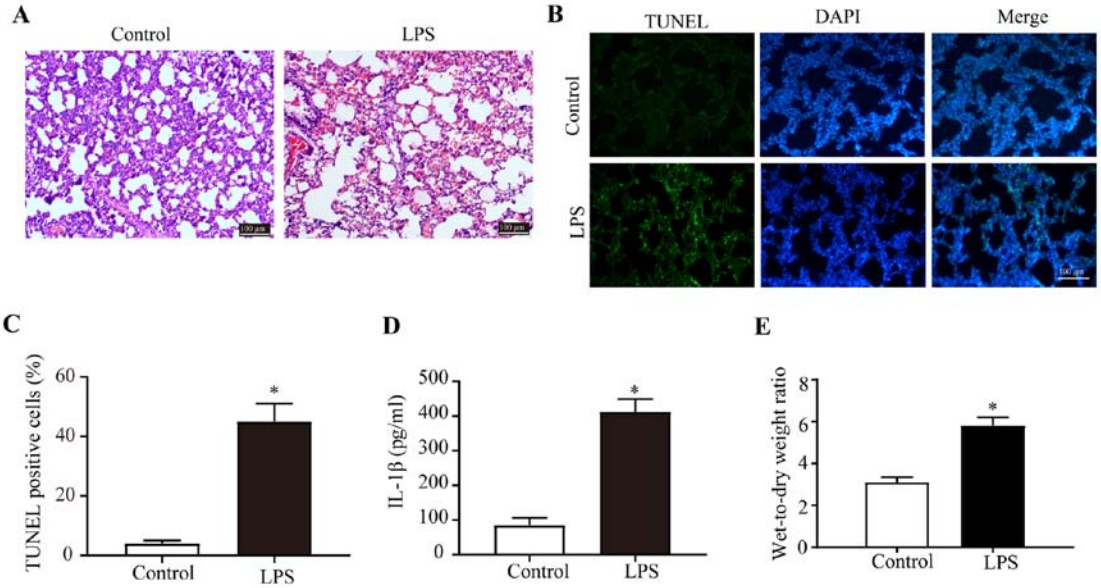

Figure 1. LPS exposure induces ALI. (A) Haematoxylin and eosin staining was performed on transverse sections of the rat lungs in the control and LPS-treated groups. (B) TUNEL staining was performed on transverse sections of the rat lungs from the control and LPS-treated groups. (C) TUNEL$^+$ cells/total cells on lung tissue between the control group and LPS-treated group. (D) ELISA results of the secretion of IL-1β in the lungs of the control or LPS-treated rats. (E) Wet-to-dry weight ratio. Scale bar, 100 μm. *P<0.05 vs. control. LSP, lipopolysaccharide; ALI, acute lung injury; IL, interleukin.

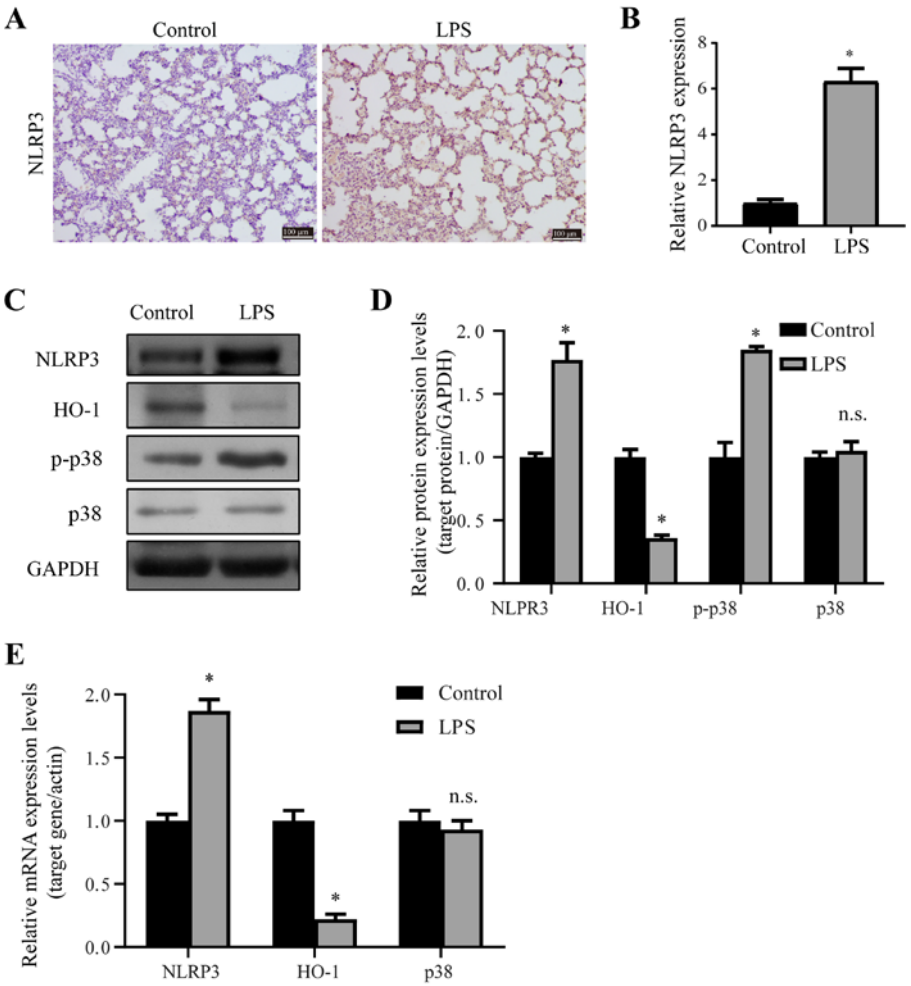

Figure 2. p38/HO-1 signaling pathway is involved in the regulation of LPS-induced ALI. (A and B) NLRP3 immunohistochemistry staining was performed on the transverse sections of rat lungs from the control and LPS-treated groups. (C and D) Western blotting results of the relative protein expression levels of NLRP3, HO-1, p-p38 and p38 in rat lungs from the control and LPS-treated group. (E) Reverse transcription-quantitative PCR results comparing the relative mRNA expression of NLRP3, HO-1 and p38 in the lungs of the control or LPS-treated rats. Scale bar, 100 μm. *P<0.05 vs. control. n.s., no significant differences; p-, phosphorylated; NLRP3, NOD-like receptor protein 3; HO-1, Heme oxygenase 1; LSP, lipopolysaccharide; ALI, acute lung injury.

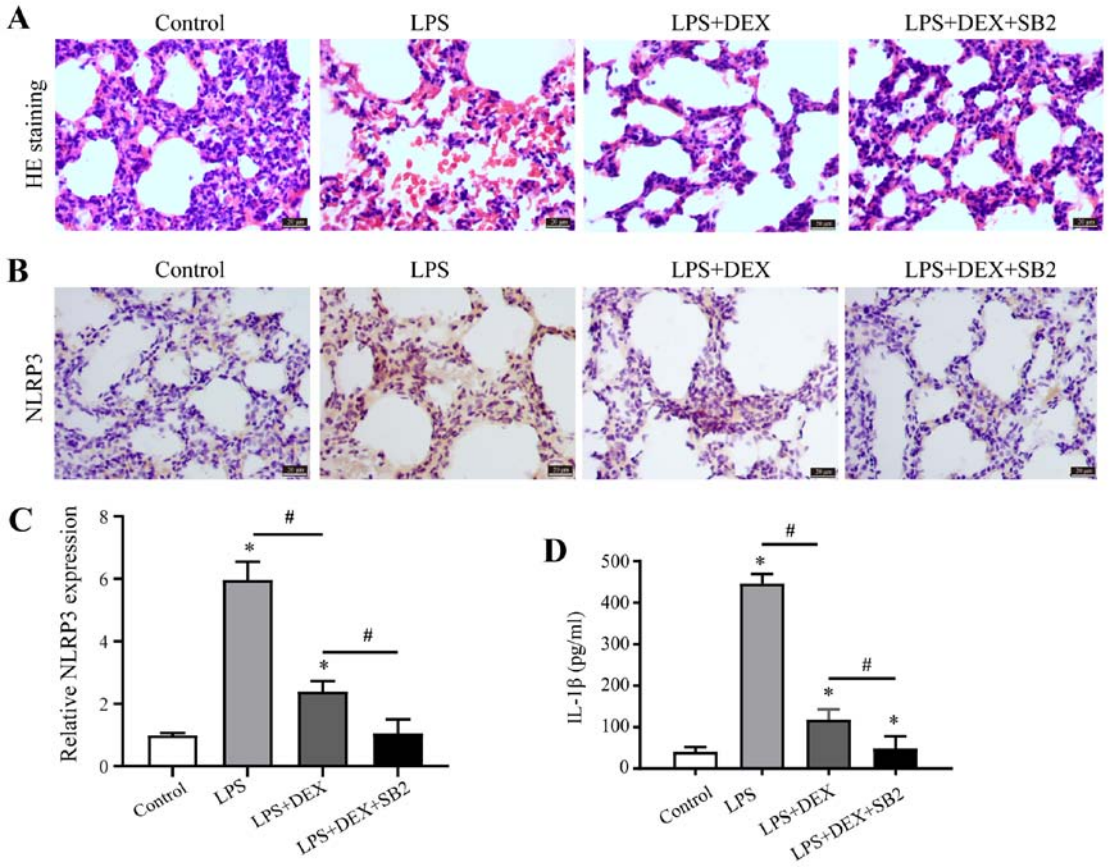

Figure 3. Dex and p38 inhibition alleviate ALI. (A) H&E staining was performed on transverse sections of the rat lungs from the control group, LPS-treated group, LPS + Dex-treated group, and the LPS + Dex + SB203580-treated group. (B and C) NLRP3 immunohistochemistry staining was performed on the transverse sections of rat lungs from the control group, LPS-treated groups, LPS + Dex-treated group, and the LPS + Dex + SB203580-treated group. (D) IL-1β immunolabeling intensities (IL-1β$^+$ cells) in lung tissue from the control group, LPS-treated groups, LPS + Dex-treated group, and the LPS + Dex + SB203580-treated group. Scale bar, 50 μm. *P<0.05 vs. control; $^\#$P<0.05 vs. LPS + Dex group. Dex, dexmedetomidine; IL, interleukin; LSP, lipopolysaccharide; ALI, acute lung injury; H&E, haematoxylin and eosin.

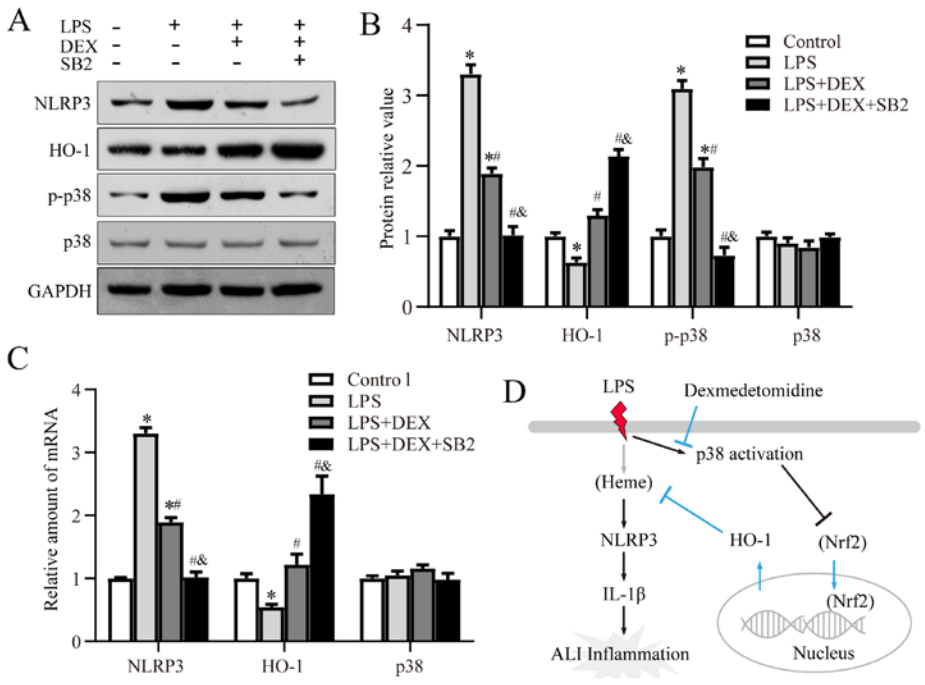

Figure 4. Dex alleviates ALI via inhibition of p38. (A and B) Western blotting results of the relative protein expression levels of NLRP3, HO-1, p-p38 and p38 in rat lungs from the control, LPS-treated group, LPS + Dex-treated group, and the LPS + Dex + SB203580-treated group. (C) Reverse transcription-quantitative PCR results of the relative mRNA expression levels of NLRP3, HO-1 and p38. (D) Diagram of the proposed signaling pathway. *P<0.05 vs. control; $^\#$P<0.05 vs. LPS group; $^\&$P<0.05 vs. LPS + Dex group. p-, phosphorylated; NLRP3, NOD-like receptor protein 3; HO-1, Heme oxygenase 1; LSP, lipopolysaccharide; ALI, acute lung injury.

lungs are the underlying causes of ALI/ARDS in pediatrics. Moreover, the incidence of ALI/ARDS in sepsis is 25-50%, which remains the main cause of serious complications and mortality (46-48). In addition, a large number of clinical blood transfusions, multiple trauma and aspiration can also cause ALI/ARDS, with an incidence rate of 40, 11-25 and 9%, respectively (49,50). Sepsis can induce inflammatory cell activation, which leads to increased permeability of pulmonary capillary endothelial cells and alveolar epithelium, and a large amount of edema fluid accumulation in the alveolar and interstitial lungs (51,52). Moreover, a variety of inflammatory cells, mainly neutrophils, adhere to the surface of damaged vascular endothelial cells and further migrate to the interstitial and alveolar spaces (53). During this process, a large number of pro-inflammatory mediators, such as IL-1β, IL-6, peroxide, leukotrienes and proteases, are released, which are involved in neutrophil-mediated lung injury, alveolar degeneration, necrosis, apoptosis and alveolar collapse, causing lung dysfunction (54-56).

The Nrf2/HO-1 signaling pathway plays an important role in preventing the occurrence of ALI/ARDS, and activation of Nrf2 prevents or reduces the severity of ALI/ARDS (26). Furthermore, activated Nrf2 is translocated into the nucleus to regulate the expression of HO-1-related genes. The activated HO-1 gene can inhibit the inflammatory cascade, thus protecting organ function and reducing ALI caused by inflammation (57). Previous studies have also reported that activation of the Nrf2/HO-1 signaling pathway inhibits the activation of NLRP3 inflammasome, thus reducing IL-1β expression and exerting anti-inflammatory and cytoprotective effects (58-60). Furthermore, HO-1 expression attenuates NLRP3 inflammasome activation (61), and multiple HO-1 inducers regulate HO-1 gene expression via ≥1 MAPK subtype signal chains (62). In the MAPK family, p38 signal transduction pathway can modulate the expression of HO-1, however, whether it promotes or inhibits the expression of HO-1 remains controversial. Previous studies have revealed that there is relationship between p38, Nrf2 and HO-1, which is characterized by sequential activation (62-64). Kim *et al* (65) reported that glycyrrhizin could activate p38, following which the expression of HO-1 increased via Nrf2, which could significantly reduce the secretion of inflammatory factors in sepsis. It has also been demonstrated that p38 can inhibit Nrf2/HO-1 gene expression. Furthermore, inhibition or genetic deficiency of p38 upregulates HO-1 via Nrf2 in monocytic cells (45) and in human hepatoma HepG2 cells (66,67). The present results also suggested that LPS stimulated p38 activation to suppress the expression of HO-1 to induce inflammation.

p38 has attracted increased attention in inflammation, and p38 kinase plays a central role in inflammatory responses (29-31). Moreover, inhibition of p38 activation has been demonstrated to suppress LPS-induced inflammation (29,33-35). The present results indicated that LPS exposure caused severe damage in rat lungs by examination of pathological tissue sections. After LPS exposure, diffuse damage was observed in the alveoli, alveolar sacs, alveolar tubes, alveolar septa and bronchi, and there were a considerable number of inflammatory cells in the alveolar septa of the LPS group. Furthermore, the increase of $TUNEL^+$ pulmonary cells in lungs and secretion levels of IL-1β also indicated that the LPS-induced ALI model was successful. It was also demonstrated that the HO-1 signaling pathway was involved in the regulation of NLRP3 via p38 in ALI. Dex has an analgesic effect and is widely used for sedation and anesthesia in patients on ICU ventilator support (68-70). However, the role of Dex in the progression of ALI is not fully understood. The current results suggested that Dex could inhibit ALI by suppressing p38 activation and activating the HO-1 signaling pathway to inhibit the LPS-induced inflammatory response.

In conclusion, the present study investigated the effect of Dex on decreasing lung inflammation in the neonatal rat LPS-induced ALI model, which may provide a theory for the pathogenesis of septic lung injury in infants and young pediatric patients. Furthermore, the results indicated that Dex functions via the p38/HO-1 and NLRP3/IL-1β signaling pathways, which may be a possible mechanism of Dex intervention in ALI. Thus, the current study provides a theoretical basis for the use of Dex in clinical patients with ALI, providing novel evidence for the discovery of new targets for clinical treatment of ALI.

Acknowledgements

Not applicable.

Funding

This work was supported by Natural Science Foundation of Anhui Province, China (grant no. 1808085MH230).

Availability of data and materials

The analyzed datasets generated during the study are available from the corresponding author on reasonable request.

Authors' contributions

YS and XY conceived and designed the present study, and provided administrative support. XY was involved in provision of study materials. YS, YX, XL and JL collected and assembled data. YS, WH and HY analyzed and interpreted the data. All authors read and approved the final manuscript.

Ethics approval and consent to participate

Not applicable.

Patient consent for publication

Not applicable.

Competing interests

The authors declare that they have no competing interests.

References

1. Hughes KT and Beasley MB: Pulmonary manifestations of acute lung injury: More than just diffuse alveolar damage. Arch Pathol Lab Med 141: 916-922, 2017.
2. Dias-Freitas F, Metelo-Coimbra C and Roncon-Albuquerque R Jr: Molecular mechanisms underlying hyperoxia acute lung injury. Respir Med 119: 23-28, 2016.

3. Monsel A, Zhu YG, Gudapati V, Lim H and Lee JW: Mesenchymal stem cell derived secretome and extracellular vesicles for acute lung injury and other inflammatory lung diseases. Expert Opin Biol Ther 16: 859-871, 2016.
4. Walkey AJ, Kirkpatrick AR and Summer RS: Systemic inflammatory response syndrome criteria for severe sepsis. N Engl J Med 373: 880, 2015.
5. Kaukonen KM, Bailey M and Bellomo R: Systemic inflammatory response syndrome criteria for severe sepsis. N Engl J Med 373: 881, 2015.
6. Khemani RG, Smith LS, Zimmerman JJ and Erickson S; Pediatric Acute Lung Injury Consensus Conference Group: Pediatric acute respiratory distress syndrome: Definition, incidence, and epidemiology: Proceedings from the pediatric acute lung injury consensus conference. Pediatr Crit Care Med 16 (5 Suppl 1): S23-S40, 2015.
7. Shi T, McAllister DA, O'Brien KL, Simoes EAF, Madhi SA, Gessner BD, Polack FP, Balsells E, Acacio S, et al: Global, regional, and national disease burden estimates of acute lower respiratory infections due to respiratory syncytial virus in young children in 2015: a systematic review and modelling study. Lancet 390: 946-958, 2017.
8. Zhou T and Chen YL: The functional mechanisms of miR-30b-5p in acute lung injury in children. Med Sci Monit 25: 40-51, 2019.
9. Shein SL, Karam O, Beardsley A, Karsies T, Prentice E, Tarquinio KM and Willson DF; Pediatric Acute Lung Injury and Sepsis Investigator (PALISI) Network: Development of an antibiotic guideline for children with suspected ventilator-associated infections. Pediatr Crit Care Med 20: 697-706, 2019.
10. Piñero P, Juanola O, Caparrós E, Zapater P, Giménez P, González-Navajas JM, Such J and Francés R: Toll-like receptor polymorphisms compromise the inflammatory response against bacterial antigen translocation in cirrhosis. Sci Rep 7: 46425, 2017.
11. Byczkowski JZ and Channel SR: Chemically-induced oxidative stress and tumorigenesis: Effects on signal transduction and cell proliferation. Toxic Subst Mechan 15: 101-128, 1996.
12. Zhang G, Li J, Xie R, Fan X, Liu Y, Zheng S, Ge Y and Chen PR: Bioorthogonal chemical activation of kinases in living systems. ACS Cent Sci 2: 325-331, 2016.
13. Sun Y, Liu J, Yuan X and Li Y: Effects of dexmedetomidine on emergence delirium in pediatric cardiac surgery. Minerva Pediatr 69: 165-173, 2017.
14. Zhang A, Pan W, Lv J and Wu H: Protective effect of amygdalin on LPS-induced acute lung injury by inhibiting NF-κB and NLRP3 signaling pathways. Inflammation 40: 745-751, 2017.
15. Zhang B, Wang B, Cao S, Wang Y and Wu D: Silybin attenuates LPS-induced lung injury in mice by inhibiting NF-κB signaling and NLRP3 activation. Int J Mol Med 39: 1111-1118, 2017.
16. Zhang A, Wang S, Zhang J and Wu H: Genipin alleviates LPS-induced acute lung injury by inhibiting NF-κB and NLRP3 signaling pathways. Int Immunopharmacol 38: 115-119, 2016.
17. Li W, Li W, Zang L, Liu F, Yao Q, Zhao J, Zhi W and Niu X: Fraxin ameliorates lipopolysaccharide-induced acute lung injury in mice by inhibiting the NF-κB and NLRP3 signalling pathways. Int Immunopharmacol 67: 1-12, 2019.
18. Gaidt MM and Hornung V: The NLRP3 inflammasome renders cell death pro-inflammatory. J Mol Biol 430: 133-141, 2018.
19. Kim JK, Jin HS, Suh HW and Jo EK: Negative regulators and their mechanisms in NLRP3 inflammasome activation and signaling. Immunol Cell Biol 95: 584-592, 2017.
20. Liu X, Pichulik T, Wolz OO, Dang TM, Stutz A, Dillen C, Delmiro Garcia M, Kraus H, Dickhöfer S, Daiber E, *et al*: Human NACHT, LRR, and PYD domain-containing protein 3 (NLRP3) inflammasome activity is regulated by and potentially targetable through bruton tyrosine kinase. J Allergy Clin Immunol 140: 1054-1067.e10, 2017.
21. Hughes FM Jr, Kennis JG, Youssef MN, Lowe DW, Shaner BE and Purves JT: The NACHT, LRR and PYD domains-containing protein 3 (NLRP3) inflammasome mediates inflammation and voiding dysfunction in a lipopolysaccharide-induced rat model of cystitis. J Clin Cell Immunol 7: 396, 2016.
22. Martinon F, Burns K and Tschopp J: The inflammasome: A molecular platform triggering activation of inflammatory caspases and processing of proIL-beta. Mol Cell 10: 417-426, 2002.
23. Lee J, Wan J, Lee L, Peng C, Xie H and Lee C: Study of the NLRP3 inflammasome component genes and downstream cytokines in patients with type 2 diabetes mellitus with carotid atherosclerosis. Lipids Health Dis 16: 217, 2017.
24. Li Y, Li N, Yan Z, Li H, Chen L, Zhang Z, Fan G, Xu K and Li Z: Dysregulation of the NLRP3 inflammasome complex and related cytokines in patients with multiple myeloma. Hematology 21: 144-151, 2016.
25. Ishii T and Mann GE: Redox status in mammalian cells and stem cells during culture in vitro: Critical roles of Nrf2 and cystine transporter activity in the maintenance of redox balance. Redox Biol 2: 786-794, 2014.
26. Rojo de la Vega M, Dodson M, Gross C, Mansour HM, Lantz RC, Chapman E, Wang T, Black SM, Garcia JG and Zhang DD: Role of Nrf2 and autophagy in acute lung injury. Curr Pharmacol Rep 2: 91-101, 2016.
27. Luo YP, Jiang L, Kang K, Fei DS, Meng XL, Nan CC, Pan SH, Zhao MR and Zhao MY: Hemin inhibits NLRP3 inflammasome activation in sepsis-induced acute lung injury, involving heme oxygenase-1. Int Immunopharmacol 20: 24-32, 2014.
28. Gao Z, Han Y, Hu Y, Wu X, Wang Y, Zhang X, Fu J, Zou X, Zhang J, Chen X, *et al*: Targeting HO-1 by epigallocatechin-3-gallate reduces contrast-induced renal injury via anti-oxidative stress and anti-inflammation pathways. PLoS One 11: e0149032, 2016.
29. Dong N, Xu X, Xue C, Wang C, Li X, Bi C and Shan A: Ethyl pyruvate inhibits LPS induced IPEC-J2 inflammation and apoptosis through p38 and ERK1/2 pathways. Cell Cycle 18: 2614-2628, 2019.
30. Xin L, Che B, Zhai B, Luo Q, Zhang C, Wang J, Wang S, Fan G, Liu Z, Feng J and Zhang Z: 1,25-Dihydroxy vitamin D3 attenuates the oxidative stress-mediated inflammation induced by PM2.5via the p38/NF-κB/NLRP3 pathway. Inflammation 42: 702-713, 2019.
31. Bailey KA, Moreno E, Haj FG, Simon SI and Passerini AG: Mechanoregulation of p38 activity enhances endoplasmic reticulum stress-mediated inflammation by arterial endothelium. FASEB J 33: 12888-12899, 2019.
32. Schieven GL: The biology of p38 kinase: A central role in inflammation. Curr Top Med Chem 5: 921-928, 2005.
33. Zhou LF, Chen QZ, Yang CT, Fu ZD, Zhao ST, Chen Y, Li SN, Liao L, Zhou YB, Huang JR and Li JH: TRPC6 contributes to LPS-induced inflammation through ERK1/2 and p38 pathways in bronchial epithelial cells. Am J Physiol Cell Physiol 314: C278-C288, 2018.
34. Abarikwu SO: Kolaviron, a natural flavonoid from the seeds of Garcinia kola, reduces LPS-induced inflammation in macrophages by combined inhibition of IL-6 secretion, and inflammatory transcription factors, ERK1/2, NF-κB, p38, Akt, p-c-JUN and JNK. Biochim Biophys Acta 1840: 2373-2381, 2014.
35. Haddad EB, Birrell M, McCluskie K, Ling A, Webber SE, Foster ML and Belvisi MG: Role of p38 MAP kinase in LPS-induced airway inflammation in the rat. Br J Pharmacol 132: 1715-1724, 2001.
36. Ayala TS, Tessaro FHG, Jannuzzi GP, Bella LM, Ferreira KS and Martins JO: High glucose environments interfere with bone marrow-derived macrophage inflammatory mediator release, the TLR4 pathway and glucose metabolism. Sci Rep 9: 11447, 2019.
37. Perrone M, Moon BS, Park HS, Laquintana V, Jung JH, Cutrignelli A, Lopedota A, Franco M, Kim SE, Lee BC and Denora N: A novel PET imaging probe for the detection and monitoring of translocator protein 18 kDa expression in pathological disorders. Sci Rep 6: 20422, 2016.
38. Herriges M and Morrisey EE: Lung development: Orchestrating the generation and regeneration of a complex organ. Development 141: 502-513, 2014.
39. Plosa EJ, Young LR, Gulleman PM, Polosukhin VV, Zaynagetdinov R, Benjamin JT, Im AM, van der Meer R, Gleaves LA, Bulus N, *et al*: Epithelial β1 integrin is required for lung branching morphogenesis and alveolarization. Development 141: 4751-4762, 2014.
40. He MY, Wang G, Han SS, Li K, Jin Y, Liu M, Si ZP, Wang J, Liu GS and Yang X: Negative impact of hyperglycaemia on mouse alveolar development. Cell Cycle 17: 80-91, 2018.
41. Chi W, Li F, Chen H, Wang Y, Zhu Y, Yang X, Zhu J, Wu F, Ouyang H, Ge J, *et al*: Caspase-8 promotes NLRP1/NLRP3 inflammasome activation and IL-1β production in acute glaucoma. Proc Natl Acad Sci USA 111: 11181-11186, 2014.
42. Suzuki H, Kanamaru K, Tsunoda H, Inada H, Kuroki M, Sun H, Waga S and Tanaka T: Heme oxygenase-1 gene induction as an intrinsic regulation against delayed cerebral vasospasm in rats. J Clin Invest 104: 59-66, 1999.
43. Jiang L and Tang Z: Expression and regulation of the ERK1/2 and p38 MAPK signaling pathways in periodontal tissue remodeling of orthodontic tooth movement. Mol Med Rep 17: 1499-1506, 2018.

44. Livak KJ and Schmittgen TD: Analysis of relative gene expression data using real-time quantitative PCR and the 2(-Delta Delta C(T)) method. Methods 25: 402-408, 2001.
45. Naidu S, Vijayan V, Santoso S, Kietzmann T and Immenschuh S: Inhibition and genetic deficiency of p38 MAPK up-regulates heme oxygenase-1 gene expression via Nrf2. J Immunol 182: 7048-7057, 2009.
46. Bosmann M and Ward PA: The inflammatory response in sepsis. Trends Immunol 34: 129-136, 2013.
47. Rice TC, Pugh AM, Caldwell CC and Schneider BSP: Balance between the proinflammatory and anti-inflammatory immune responses with blood transfusion in sepsis. Crit Care Nurs Clin North Am 29: 331-340, 2017.
48. Kaukonen KM, Bailey M, Pilcher D, Cooper DJ and Bellomo R: Systemic inflammatory response syndrome criteria in defining severe sepsis. N Engl J Med 372: 1629-1638, 2015.
49. Chang M, Lu HY, Xiang H and Lan HP: Clinical effects of different ways of mechanical ventilation combined with pulmonary surfactant in treatment of acute lung injury/acute respiratory distress syndrome in neonates: A comparative analysis. Zhongguo Dang Dai Er Ke Za Zhi 18: 1069-1074, 2016 (In Chinese).
50. Chaiwat O, Chittawatanarat K, Piriyapathsom A, Pisitsak C, Thawitsri T, Chatmongkolchart S and Kongsayreepong S: Incidence of and risk factors for acute respiratory distress syndrome in patients admitted to surgical intensive care units: The multicenter thai University-based surgical intensive care unit (THAI-SICU) study. J Med Assoc Thai 99 (Suppl 6): S118-S127, 2016.
51. Gong Y, Lan H, Yu Z, Wang M, Wang S, Chen Y, Rao H, Li J, Sheng Z and Shao J: Blockage of glycolysis by targeting PFKFB3 alleviates sepsis-related acute lung injury via suppressing inflammation and apoptosis of alveolar epithelial cells. Biochem Biophys Res Commun 491: 522-529, 2017.
52. Zhang X and Dong S: Protective effects of erythropoietin towards acute lung injuries in rats with sepsis and its related mechanisms. Ann Clin Lab Sci 49: 257-264, 2019.
53. Wygrecka M, Jablonska E, Guenther A, Preissner KT and Markart P: Current view on alveolar coagulation and fibrinolysis in acute inflammatory and chronic interstitial lung diseases. Thromb Haemost 99: 494-501, 2008.
54. Lim R, Barker G and Lappas M: TLR2, TLR3 and TLR5 regulation of pro-inflammatory and pro-labour mediators in human primary myometrial cells. J Reprod Immunol 122: 28-36, 2017.
55. Jin Z, Yang YZ, Chen JX and Tang YZ: Inhibition of pro-inflammatory mediators in RAW264.7 cells by 7-hydroxyflavone and 7,8-dihydroxyflavone. J Pharm Pharmacol 69: 865-874, 2017.
56. Lappas M: The IL-1β signalling pathway and its role in regulating pro-inflammatory and pro-labour mediators in human primary myometrial cells. Reprod Biol 17: 333-340, 2017.
57. Feng G, Sun B, Liu HX, Liu QH, Zhao L and Wang TL: EphA2 antagonism alleviates LPS-induced acute lung injury via Nrf2/HO-1, TLR4/MyD88 and RhoA/ROCK pathways. Int Immunopharmacol 72: 176-185, 2019.
58. Chen Z, Zhong H, Wei J, Lin S, Zong Z, Gong F, Huang X, Sun J, Li P, Lin H, *et al*: Inhibition of Nrf2/HO-1 signaling leads to increased activation of the NLRP3 inflammasome in osteoarthritis. Arthritis Res Ther 21: 300, 2019.
59. Mahmoud AM, Hussein OE, Abd El-Twab SM and Hozayen WG: Ferulic acid protects against methotrexate nephrotoxicity via activation of Nrf2/ARE/HO-1 signaling and PPARγ, and suppression of NF-κB/NLRP3 inflammasome axis. Food Funct 10: 4593-4607, 2019.
60. Liu S, Tian L, Chai G, Wen B and Wang B: Targeting heme oxygenase-1 by quercetin ameliorates alcohol-induced acute liver injury via inhibiting NLRP3 inflammasome activation. Food Funct 9: 4184-4193, 2018.
61. Xiaoyu H, Si H, Li S, Wang W, Guo J, Li Y, Cao Y, Fu Y and Zhang N: Induction of heme oxygenas-1 attenuates NLRP3 inflammasome activation in lipopolysaccharide-induced mastitis in mice. Int Immunopharmacol 52: 185-190, 2017.
62. Zhang X, Xu X, Yu Y, Chen C, Wang J, Cai C and Guo W: Integration analysis of MKK and MAPK family members highlights potential MAPK signaling modules in cotton. Sci Rep 6: 29781, 2016.
63. Roux PP and Blenis J: ERK and p38 MAPK-activated protein kinases: A family of protein kinases with diverse biological functions. Microbiol Mol Biol Rev 68: 320-344, 2004.
64. Wagner EF and Nebreda AR: Signal integration by JNK and p38 MAPK pathways in cancer development. Nat Rev Cancer 9: 537-549, 2009.
65. Kim YM, Kim HJ and Chang KC: Glycyrrhizin reduces HMGB1 secretion in lipopolysaccharide-activated RAW 264.7 cells and endotoxemic mice by p38/Nrf2-dependent induction of HO-1. Int Immunopharmacol 26: 112-118, 2015.
66. Keum YS, Yu S, Chang PP, Yuan X, Kim JH, Xu C, Han J, Agarwal A and Kong AN: Mechanism of action of sulforaphane: Inhibition of p38 mitogen-activated protein kinase isoforms contributing to the induction of antioxidant response element-mediated heme oxygenase-1 in human hepatoma HepG2 cells. Cancer Res 66: 8804-8813, 2006.
67. Yu R, Mandlekar S, Lei W, Fahl WE, Tan TH and Kong AN: p38 mitogen-activated protein kinase negatively regulates the induction of phase II drug-metabolizing enzymes that detoxify carcinogens. J Biol Chem 275: 2322-2327, 2000.
68. Venkatraman R, Hungerford JL, Hall MW, Moore-Clingenpeel M and Tobias JD: Dexmedetomidine for sedation during noninvasive ventilation in pediatric patients. Pediatr Crit Care Med 18: 831-837, 2017.
69. Sottas CE and Anderson BJ: Dexmedetomidine: The new all-in-one drug in paediatric anaesthesia? Curr Opin Anaesthesiol 30: 441-451, 2017.
70. Devasya A and Sarpangala M: Dexmedetomidine: A review of a newer sedative in dentistry. J Clin Pediatr Dent 39: 401-409, 2015.